JOURNAL OF GEOPHYSICAL RESEARCH, VOL. 100, NO. D4, PAGES 7203–7221, APRIL 20, 1995

Carbon-biosphere-climate interactions in the last glacial maximum climate

P. Friedlingstein
Belgian Institute for Space Aeronomy, Brussels, Belgium

K. C. Prentice, I. Y. Fung, and J. G. John
NASA Goddard Institute for Space Studies, New York

G. P. Brasseur
National Center for Atmospheric Research, Boulder, Colorado

Abstract. The total carbon inventory in the terrestrial biosphere in the last glacial maximum (LGM), 18 kyr ago, is analyzed in a series of experiments that examine the sensitivity of the inventory to vegetation distribution and carbon dynamics. The results show that for most forest vegetation types, carbon densities for the LGM are within 10% of their present-day values. Discrepancies between vegetation distributions simulated by two bioclimatic schemes are attributable to the assignation of vegetation types to climates with rare or no present-day analog. The model experiments, combined with palynogical data for regions with no present-day analog climate, yield to a decrease of 612 ± 105 Gt C compared to present day.

Introduction

Principles that guide the contemporary distribution of vegetation on the globe and the redistribution of vegetation under different climates have not been fully understood. Projections of changes have thus relied on bioclimatic associations that define the ranges in climate space for each vegetation habitat [*Manabe and Stouffer*, 1980; *Hansen et al.*, 1984; *Emanuel et al.*, 1985]. The commonly used schemes are the *Holdridge* [1947] and *Köppen* [1936] schemes. As the associations are developed for present-day conditions, the validity of their application to altered climates has not been established.

Validation of any bioclimatic scheme for altered climate conditions is difficult. The very nature of the fossil record on flora and fauna is more appropriate for the investigation on temporal changes at a particular site rather than mapping spatial variations for a single period. Furthermore, uncertainties in the dating of the fossil records, the translation of pollen data to species information and then into the biome nomenclature used in the modeling schemes, the spatial representativeness of site data, the assumption of equilibrium between climate and vegetation all introduce unquantifiable uncertainties into the comparison between empirical and modeled vegetation distribution. For the last glacial maximum (LGM), vegetation distributions have been compiled by *Climate: Long-Range Investigation Mapping and Prediction (CLIMAP)* [1976] and more recently by *Adams et al.* [1990], *Frenzel et al.* [1992], or *Vancampo et al.* [1993]. Although recent advances in global scale biospheric modeling have resulted in prognostic schemes that include aspects of plant physiology to define the climate range for the survival of particular vegetation types [e.g., *Woodward*, 1987; *Prentice et al.*, 1992], there has been no systematic attempt to understand the divergences between the reconstructions or with the distributions modeled for the same period [*Hansen et al.*, 1984; *Prentice and Fung*, 1990; *Friedlingstein et al.*, 1992; *Esser and Lautenschlager*, 1994].

Changes in vegetation distribution may be accompanied by a change in global carbon inventory of the terrestrial biosphere. Because independent information exists for changes in the carbon inventory of the atmospheric and oceanic reservoirs, estimates of terrestrial carbon changes may provide a global rather than local or regional cross-check on the modeled vegetation distribution. For the LGM the atmospheric CO_2 concentration of 200 part per million by volume (ppmv) has been measured in air bubbles in ice cores [*Barnola et al.*, 1987]. The glacial oceanic carbon was isotopically lighter than today. *Shackleton* [1977] first measured a $\Delta\delta^{13}C$ of 0.7 ‰ in equatorial Pacific cores between LGM and today. If one assumes that this isotopic change is due to transfer of carbon from the ocean (av-

Paper number 94JD02948.
0148-0227/95/94JD-02948$05.00

erage $\delta^{13}C \sim 0$ ‰) to the terrestrial organic reservoir (average $\delta^{13}C \sim$ -25 ‰), these data imply that the terrestrial carbon pool was 1000 Gt C lower during the LGM than today. More recently, *Duplessy et al.* [1988], analyzing Atlantic and Pacific cores, updated this estimation and reduced the $\Delta\delta^{13}C$ to a global mean value of 0.32 ‰. In a recent review of the glacial–Holocene transition, *Broecker and Peng* [1993] also suggest a 0.3 to 0.4 ‰ shift in the $\delta^{13}C$ oceanic record. Using the mean value of 0.35 ‰, they infer the following carbon budget (in gigatonnes of carbon):

	LGM	Holocene	Change
Ocean	35740	35100	- 640
Atmosphere	360	500	+ 140
Biosphere	1500	2000	+ 500

If one includes the 0.1 ‰ uncertainty in the $\Delta\delta^{13}C$, the inferred biospheric change ranges from 425 to 665 GtC.

By contrast, direct estimates of terrestrial carbon inventories show a range of no change [*Prentice and Fung,* 1990 (hereinafter referred to as PF90)] to 300 GtC [*Friedlingstein et al.,* 1992 (hereinafter referred to as F92)] to 1300 GtC [*Adams et al.,* 1990]. Reasons of these differences are mainly due to vegetation distributions. According to *Adams et al.* [1990], vegetation types associated with drier climatic conditions such as desert, grassland, and tundra were much more extended during the LGM than they are today, but forests were extremely reduced. The PF90 conclusion was basically opposite, during the LGM, deserts are dramatically reduced and forests expanded. The F92 estimate is intermediate, deserts, and grasslands, as in the work of *Adams et al.* [1990] take the lead during the LGM, but the magnitude of this shift is much more reduced.

In this paper we focus on understanding the uncertainties and sensitivities of the modeled estimates of terrestrial carbon inventories in altered climates. Because of the urgency of projections of future levels of atmospheric carbon dioxide we limit our focus on models rather than on empirical derivation of the vegetation distribution or of the carbon inventory. We reexamine the carbon stored during the LGM, focusing on the sensitivity of this estimate to the climate, vegetation, or carbon treatments.

Methodology

The strategy we employ is similar to the one used in PF90 and in F92. We start with a LGM climate simulated by a general circulation model (GCM) and use it to force bioclimatic and carbon schemes. We made use of three LGM climates, two bioclimatic schemes, and one carbon scheme in order to provide six simulations of the vegetation and terrestrial carbon reservoirs distribution at the LGM. In the following we shall denote these experiments by the climate•bioclimatic scheme.

The modeled estimations are evaluated against two classes of constraints. On a local scale, palynological data provide in situ validation of the modeled vegetation distribution, in locations where the data are available, dated, and can be interpreted with confidence as a biome shift. These are discussed further in the results section.

As mentionned in the introduction, on the global scale the change in total carbon stored on land can be inferred from the change in $\delta^{13}C$ recorded in oceanic sediments.

Climate

For the present day, global distributions of monthly mean surface air temperature and precipitation were compiled from weather station data by several investigators [*Shea,* 1986; *Legates and Willmott,* 1989; *Leemans and Cramer,* 1991]. As expected, the data sets are very similar on the large scale. The recent data sets, with their higher spatial resolution (0.5° × 0.5°) exhibit finer structure in the compiled fields. Here we use the compilation of *Shea* [1986] as our starting point for several reasons; both of the bioclimatic schemes we are testing [*Prentice,* 1990; F92] are based on this data set, and also there have been extensive comparisons between GCM simulations and *Shea* [1986].

Present-day climate as well as LGM climate were simulated using the Goddard Institute for Space Studies (GISS) GCM [*Hansen et al.,* 1984] and the Sellers [1983, 1985] three-dimensional global climate model. Because of known deficiencies in these GCMs in their simulation of the present-day climate, we calculated LGM climate anomalies from the GCMs as the departures from the corresponding present-day simulation and added the anomalies to the present-day climatology of *Shea* [1986]. In this way the GISS and Sellers LGM climates were rooted in present-day observations. These two simulated climates will be referred as GISS* LGM and Sellers* LGM hereinafter. Direct simulation of the LGM climate with the GISS model (hereinafter referred to as GISS LGM) was also used here as it is the climate actually used by PF90 (they had mistakenly reported the use of GISS* LGM.) We have thus three representations of LGM climate.

We note that there has been intense controversy over the tropical and subtropical sea surface temperatures (SSTs) inferred for the LGM [e.g., *Rind and Peteet,* 1985; *Rind,* 1989; *Anderson and Webb,* 1994]. The LGM SSTs reconstructed from the distribution of foraminifers in the ocean sediments [*CLIMAP,* 1976] imply no change in SST between the LGM and today, whereas the descent of tropical glaciers [*Porter* 1979; see also *Rind and Peteet,* 1985] would imply a decrease in SSTs in the tropics, if the atmospheric lapse rate is constant. On the other hand, $\delta^{18}O$ and Sr/Ca data recorded in Barbados corals suggest that LGM tropical SSTs were 5°C colder than today [*Guilderson et al.,* 1994]. Therefore the use of SSTs as boundary conditions for the GCM simulations inevitably transfers their uncertainties to the simulated climate.

The GISS simulations used here employ a globally uniform 2°C drop in SSTs as opposed to the CLIMAP reconstructions [*Hansen et al.,* 1984].

Bioclimatic Subschemes

The vegetation distribution was estimated with two different bioclimatic schemes. The first one [*Prentice,* 1990] is a modified Holdridge scheme, correlating present-day distribution of annual precipitation, biotemperature (mean annual temperature of months having a temperature higher than 0°C), and vegetation distribution from *Matthews* [1983]. It originally accounted for 29 vegetation types, but we have aggregated it into nine vegetation types to facilitate comparisons with the F92 bioclimatic scheme.

This latter scheme is also based on correlations between observed vegetation distribution and climate. The World ecosystem database from *Olson et al.* [1985] was used to derive nine natural vegetation types (perennial ice, desert and semidesert, tundra, coniferous forest, temperate deciduous forest, grassland and shrubland, savanna, seasonal tropical forest, and evergreen tropical forest). As in the Prentice scheme, climatology from *Shea* [1986] is used to obtain the two driving climatic variables, the annual precipitation, and the biotemperature.

Empirical relationships between the spatial distribution of each of the nine vegetation types and the two climatic variables were developed. Each vegetation type is allowed to exist within a defined domain of precipitation and biotemperature.

Carbon Dynamics Scheme

The carbon dynamics scheme used in this study is a component of the scheme for large-scale atmosphere vegetation exchange (SLAVE) [F92; *Friedlingstein et al.,* 1994]. In its entirety, SLAVE starts with a climatic distribution, determines the vegetation distribution using a bioclimatic scheme and calculates the main carbon fluxes and pools as a function of climatic variables and vegetation type. The carbon fluxes and pools are in turn modulated by the water and nutrient status of the soil and CO_2 concentration in the atmosphere. For the present study, we used both *Prentice* [1990] and F92 bioclimatic schemes described earlier. We did not include the effects of soil water and nutrient limitations on carbon dynamics or CO_2 fertilization, as the distributions of soil types and soil properties for the LGM are unknown.

The model computes the annual net primary production (NPP) using a formulation derived from the Miami model [*Lieth,* 1975; F92]. Carbon pools are hence calculated, assuming vegetation types dependent turnover times in phytomass and litter compartment (Table 1, columns 3 to 6) and a uniform turnover time for the soil pool (250 yr). Phytomass and litter pools are subdivided into herbaceous and woody compartment (Table 1, column 2).

Results and Discussion

Present-Day Simulations

Before exploring LGM climates, we simulated the present-day biosphere, using the *Shea* [1986] climatology, the Prentice and the Friedlingstein bioclimatic schemes successively, and the carbon dynamics scheme in the SLAVE model.

Global vegetation distribution patterns simulated for the present with the two bioclimatic schemes show good agreement. Grasslands, coniferous, temperate deciduous, and tropical evergreen forests surface areas produced by the two schemes differ by less than 3% (Table 2). However, the Friedlingstein scheme produces 25% less ice and 43.2 % more tundra than the Prentice scheme (expanding southward); also the agreement on savanna versus seasonal tropical forest repartition in the tropical band is weak; the Prentice scheme producing 54.3 % more seasonal forest and 25.3 % less savanna than the Friedlingstein scheme (Table 2). Part of this discrepancy is due to the vegetation type nomenclature. Indeed, when savanna and seasonal tropical forest are summed up, the disagreement falls to 16.5 %; similarly, disagreement on ice and tundra is reduced to 21% when these two types are combined. Discrepancy between the

Table 1. Vegetation Type Dependent Parameters of the SLAVE Model

	Vegetation Type	Herb Ratio	Herb Phyt Res Time	Wood Phyt Res Time	Herb Lit Res Time	Wood Lit Res Time
1	evergreen tropical forest	0.4	1.0	30.	0.2	0.5
2	seasonal tropical forest	0.4	1.0	30.	0.25	0.67
3	savanna	0.9	1.0	30.	0.25	0.67
4	grassland/shrubland	1.0	1.0	...	1.0	...
5	temperate deciduous forest	0.4	2.0	50.	1.0	5.0
6	coniferous forest	0.4	2.0	50.	2.0	6.67
7	tundra	0.85	1.5	40.	4.0	10.0
8	warm desert	1.0	1.0	...	0.33	...
9	cold desert	1.0	1.5	...	1.0	...

Fraction of herbaceous net primary production, and residence time (year) of herbaceous and woody materials in phytomass and litter. There is a temperature correction for temperate forest and seasonal tropical forest residence times: between 16°C and 22°C they linearly decrease from the temperate deciduous values to the seasonal tropical forest values listed in the table. Herb, herbaceous; Wood, woody; Phyt, phytomass; Lit, Litter; Res, Residence.

Table 2. Present-Day Vegetation Type Areas and Carbon Inventory Modeled With Prentice's and Friedlingstein's Bioclimatic Schemes

	Prentice Scheme				Friedlingstein Scheme			
Veg Type	Area, 10^6 km^2	Phyt C, Gt C	Lit C, Gt C	Soil C, Gt C	Area, 10^6 km^2	Phyt C, Gt C	Lit C, Gt C	Soil C, Gt C
1	13.0	202.1	4.7	100.9	12.4	186.0	4.0	85.2
2	12.7	137.6	4.8	96.5	5.8	67.4	2.1	43.3
3	9.1	55.6	2.7	46.7	11.9	47.6	3.0	46.0
4	36.8	63.1	10.0	144.4	36.1	39.3	10.6	140.2
5	16.8	236.8	15.3	329.4	17.2	266.8	14.2	310.0
6	20.8	191.7	20.0	418.1	20.8	205.5	22.9	476.8
7	7.4	19.8	4.3	72.5	10.6	30.4	6.7	114.2
8	13.8	3.3	0.8	11.1	16.6	1.3	0.5	6.7
9	3.6	1.2	0.3	4.7	2.7	0.2	0.1	1.1
Global	134.0	911.2	62.9	1224.2	134.0	844.4	64.1	1223.5

Units are 10^6 km^2 and GtC, respectively. Veg, vegetation.

vegetation type surface areas is also due to the different original model resolutions. Vegetation type averaged NPP, phytomass, litter, and soil densities are almost independent of the bioclimatic scheme used (Figure 1). Global biospheric carbon content amounts to 2198 GtC when the Prentice bioclimatic scheme is used and 2132 GtC with the Friedlingstein scheme. Vegetation type repartition of carbon is also primarily independent of the bioclimatic scheme (Figure 2).

Carbon Densities at the Last Glacial Maximum

LGM climate introduces a reestimation of the global carbon inventory due to a change in vegetation distribution and/or a change in carbon densities of vegetation and soil types. *Adams et al.* [1990] as well as PF90 based their calculations on the assumption that for a given vegetation type, phytomass and soil carbon densities remain constant during a climatic change. In the present study, the use of a carbon scheme (where carbon densities are not fixed a priori but deduced a posteriori from the computation of biospheric fluxes and pools driven by climate) allows us to test the assumption made by Adams et al. and by PF90. For every climate•bioclimatic scheme experiment we computed the phytomass, litter, and soil densities of each vegetation type.

Figure 3 shows relative changes (percent) of NPP, phytomass, litter and soil densities for each vegetation type under the LGM climates, relative to the corresponding densities simulated with the same bioclimatic scheme for today. As shown in this figure, these densities remain rather constant under climatic change. For high NPP vegetation types (forests), relative changes are within 10%, low NPP vegetation types (tundra, grassland, savanna) exhibit larger relative changes (20%); the same conclusion applies for phytomass density. That relative constancy can easily be explained by the "Lagrangian" approach we used, where vegetation types are redistributed according to the disturbed climate. Therefore the photosynthesis and decomposition processes which drive the biospheric pool densities are, within a given vegetation type, experiencing a climate similar to the undisturbed climate.

It should be noted that the temperate deciduous forest does not seem to follow this rule, Figure 3 showing clearly a significant decrease in litter and soil carbon densities for this vegetation type (from -8.7 % for GISS* LGM•Friedlingstein to -31.2 % for Sellers* LGM•Prentice). This may be due to the relatively broad climatic domain of this type; that is, there is still much room in its climate space to move around within its climate boundaries. This would not hold if a higher-resolution bioclimatic scheme was used.

LGM Carbon Inventory

Global estimates of the carbon inventory of the biospheric pools at LGM (Table 3, Figure 4) cover an extremely wide range, from 608 GtC less than today for Sellers* LGM•Prentice to 593 GtC more than today for GISS LGM•Friedlingstein. Figure 4 shows the relative changes (percent) of total carbon stored in each vegetation type under the LGM conditions. Part of this discrepancy is due to the LGM climate: GISS LGM is the only one that gives (no matter the bioclimatic scheme used) more carbon stored during the ice age than today, which is in complete disagreement with the $\Delta\delta^{13}$C oceanic constraint. The simulated GISS LGM climate is known to be wetter than today's climate [*Rind,* 1987]. GISS* LGM and Sellers* LGM give lower carbon content for the LGM period than today but still present very large differences. The Sellers GCM includes a simple diffusive oceanic model and hence does not need SST information as boundary conditions as GISS needs. Uncertainties in the LGM SST may explain part of the difference between these two LGM climates, Sellers* LGM being warmer and dryer than GISS* LGM (Plate 1). When different bioclimatic schemes are applied to the same LGM climate, large differences in the global carbon estimates persist.

The Prentice scheme and the Friedlingstein scheme predict, respectively, 1837 and 2114 GtC under GISS* LGM climate, 1590 and 1620 GtC under Sellers* LGM

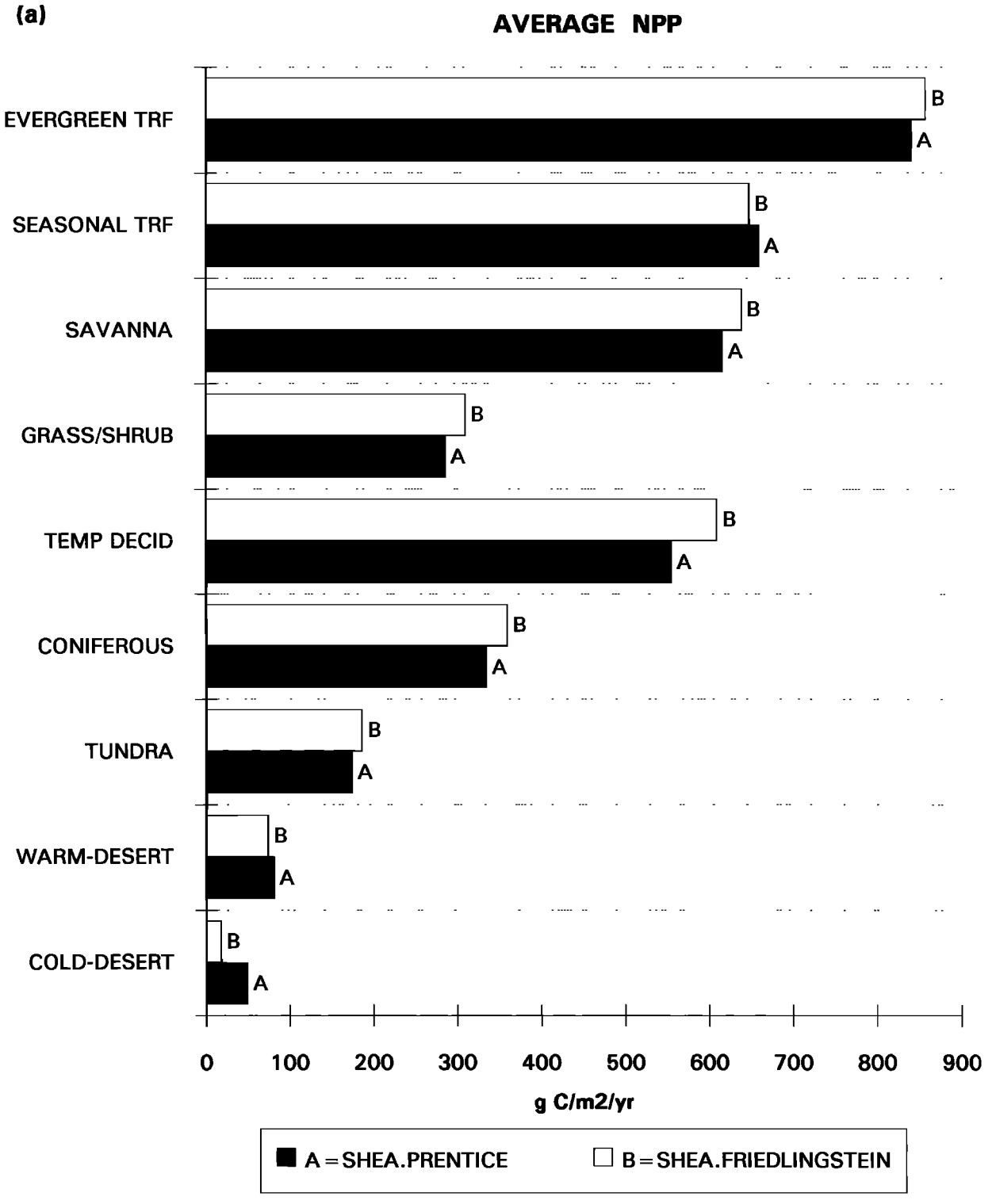

Figure 1. (a) Net primary production (NPP), and carbon densities in (b) phytomass, (c) litter, and (d) soil, averaged for nine vegetation types and for the global land surface area. The vegetation distributions were modeled with Prentice's (A) and Friedlingstein's (B) bioclimatic schemes. Unit of NPP is $gC/yr/m^2$. Unit of carbon densities is gC/m^2.

climate, and 2241 and 2725 GtC under GISS LGM climate (Table 3). For each pair of experiments the difference among phytomass, litter and soil carbon pools occurs mainly in the tropical regions, where the vegetation type distribution predicted by Prentice's or Friedlingstein's scheme differs dramatically. Particularly with the GISS GCM climate, Prentice's scheme predicts evergreen tropical forest, whereas Friedlingstein's scheme

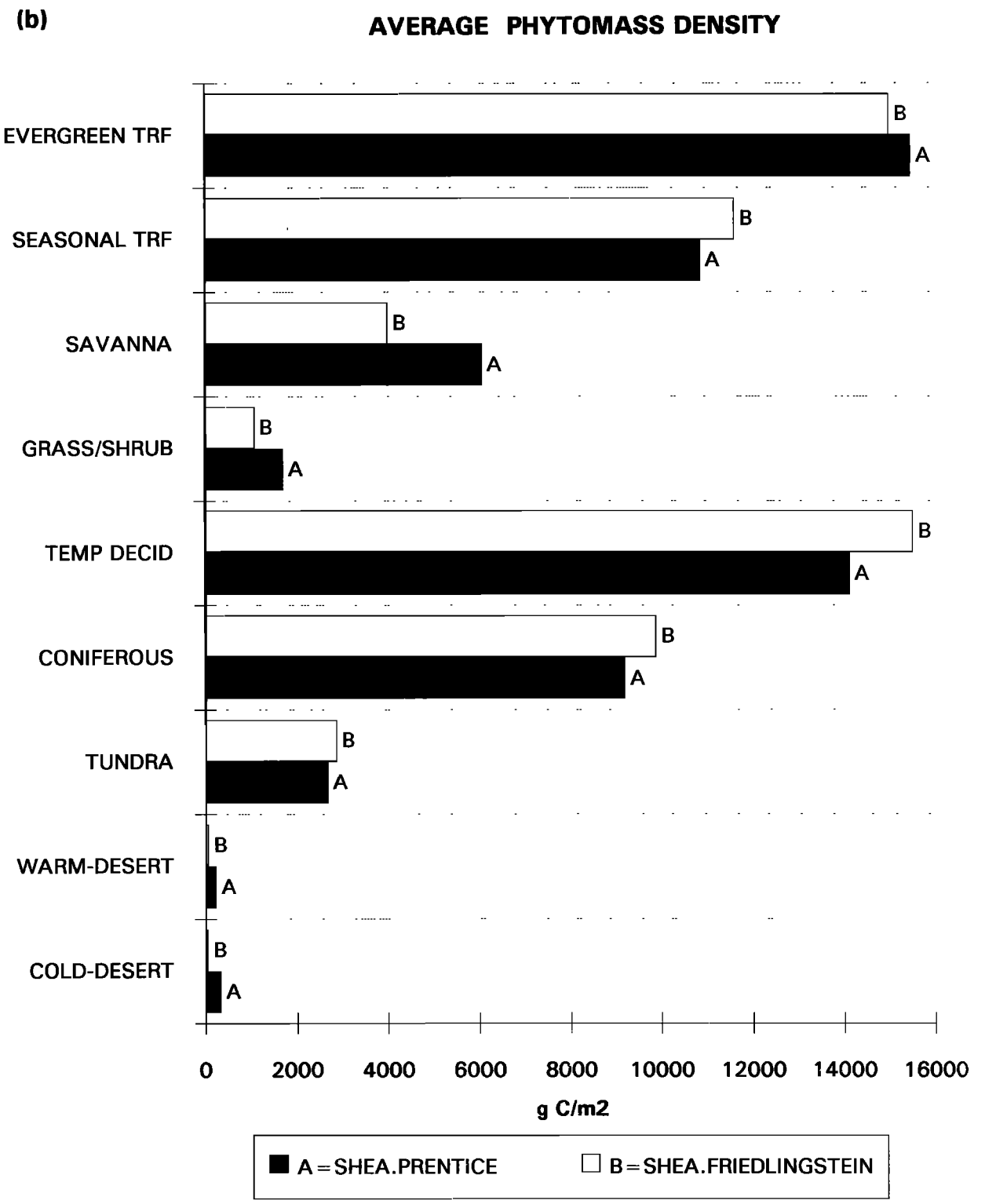

Figure 1. (continued)

produces temperate deciduous forest (the same occurs, but to a lesser extent, with GISS* LGM climate) (Table 3). The impact of these vegetation differences on the carbon estimate is very important (Figure 4). In SLAVE, residence time of carbon in biospheric reservoirs is shorter for tropical than for temperate forest (Table 1). Consequently, the LGM carbon inventory in the tropical region is always higher with the Friedlingstein scheme than with the Prentice scheme. This discrepancy between bioclimatic schemes was not expected as both schemes reproduce the present-day vegetation quite well. The climatic conditions occurring in these tropical regions where the disagreement is the most important are rarely or even never encountered in the

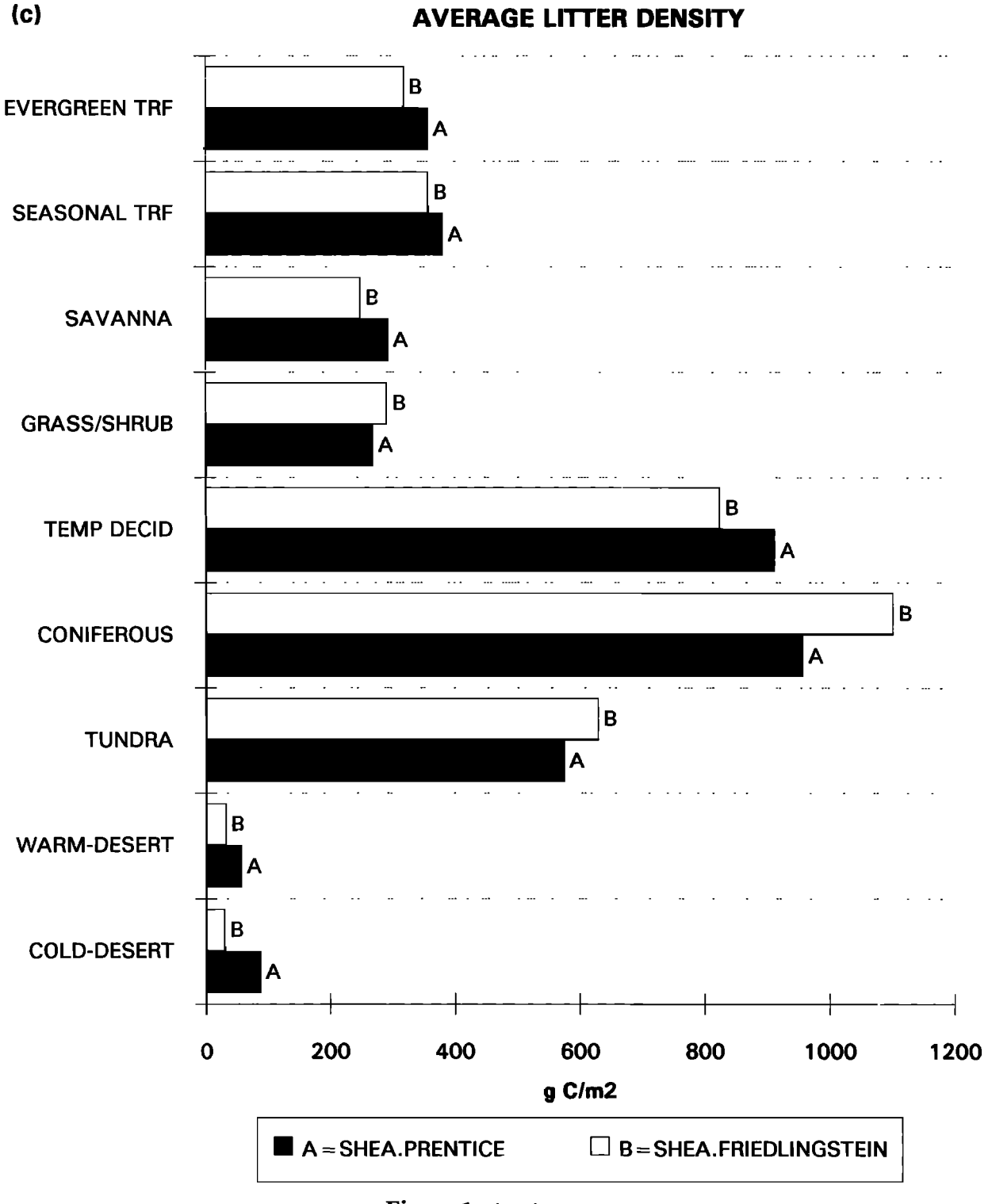

Figure 1. (continued)

today climate (Plate 1). Therefore for these climatic regimes, our confidence in any climate–vegetation relationship is weak.

To quantify our confidence in the climate–vegetation correlations, we divided the climatic space (biotemperature–annual precipitation) into 2°C x 100 mm bins and counted the occurrences of each climatic bin in the present-day climatology (at a 5° × 5° resolution, 923 land grid cells) (Plate 2). We define climates as "common", "infrequent", "rare", and "no-analog", if >4, 2-4, 1, and 0 grid cells, respectively, are in the bin under present-day conditions. These would imply high (for "common" climates), medium (for "infrequent" climates), and low (for "rare" and "no-analog" climates) confidence in the vegetation simulated as the bioclimatic models are correlative schemes. Plate 2 shows the

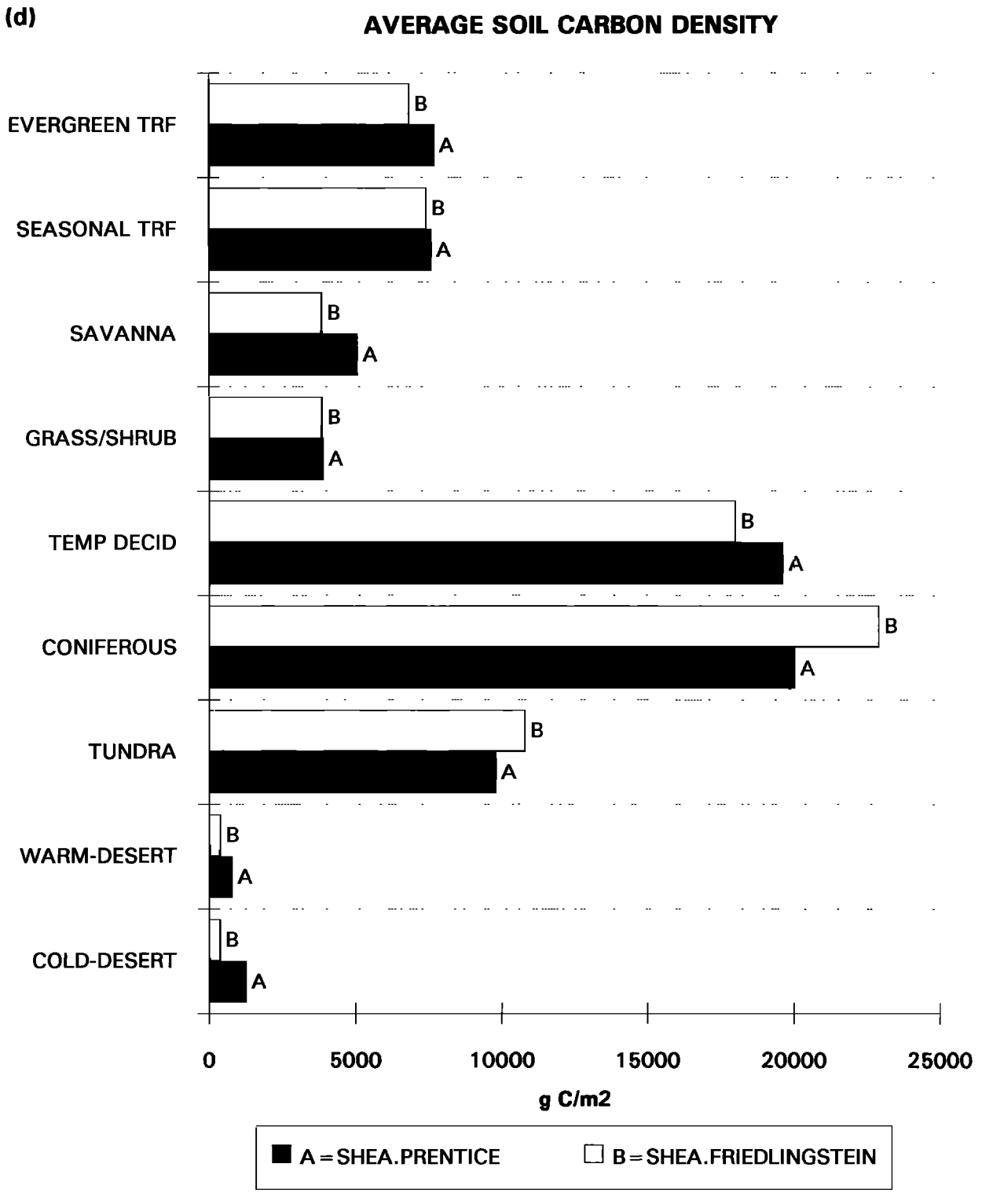

Figure 1. (continued)

geographic distribution of the regions of common, infrequent, rare, and no-analog climates for the present-day and three LGM climates. Singular climates (rarely or never encountered today) are dominant in the tropical band (orange and red regions), precisely where the two bioclimatic schemes show the weaker agreement. The vegetation predicted in these "low-confidence" regions is highly dependent on the way each bioclimatic scheme interprets vegetation for the no present-day analog climates. For a given LGM climate the global carbon estimate is dependent on the bioclimatic scheme primarily through these crucial no present-day analog regions. This pattern is clearly shown in Figure 5, where global carbon estimate in the three biospheric reservoirs has been split into the high, medium, and low-confidence regions. It is clear from this figure that the discrepancy

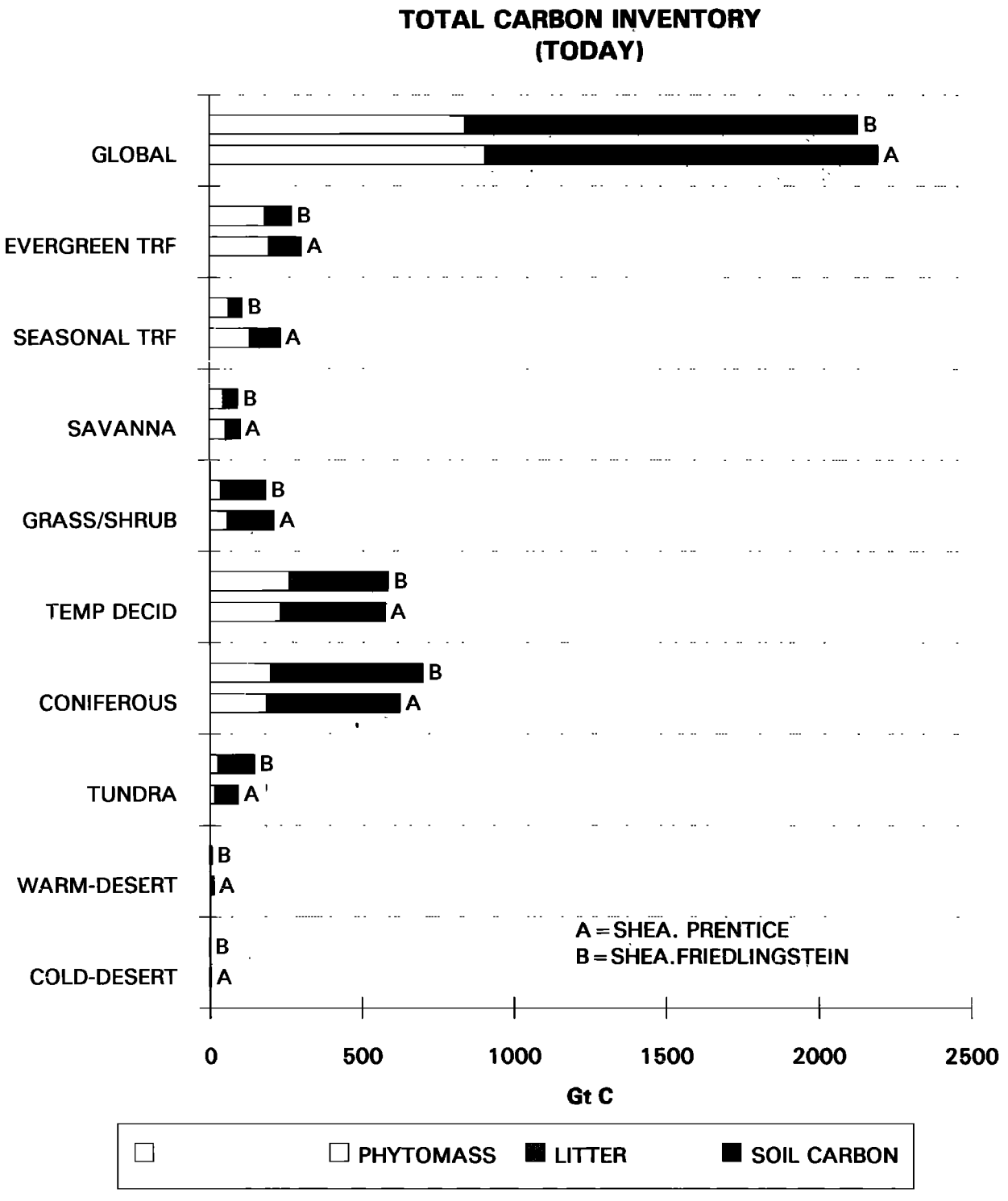

Figure 2. Present-day carbon inventories in phytomass, litter, and soil, for vegetation types modeled with Prentice's (A), and Friedlingstein's (B) bioclimatic schemes. Unit is gigatonnes of carbon.

in the carbon estimations is almost exclusively located in the low-confidence regions. In these regions, carbon estimations can differ by 40% depending on the bioclimatic scheme used, compared to maximum 10% for the medium- and high-confidence regions.

These results show the limitations of correlative bioclimatic schemes when applied to climates different from that used to develop the scheme. Bioclimatic schemes based on physiological plant processes [e.g., *Prentice et al.*, 1992; *Woodward*, 1987] may be more able to treat these no-analog climates than the correlative schemes do. It is likely that these latter may not be suitable for predicting equilibrium vegetation for future climates with large regions with no present-day

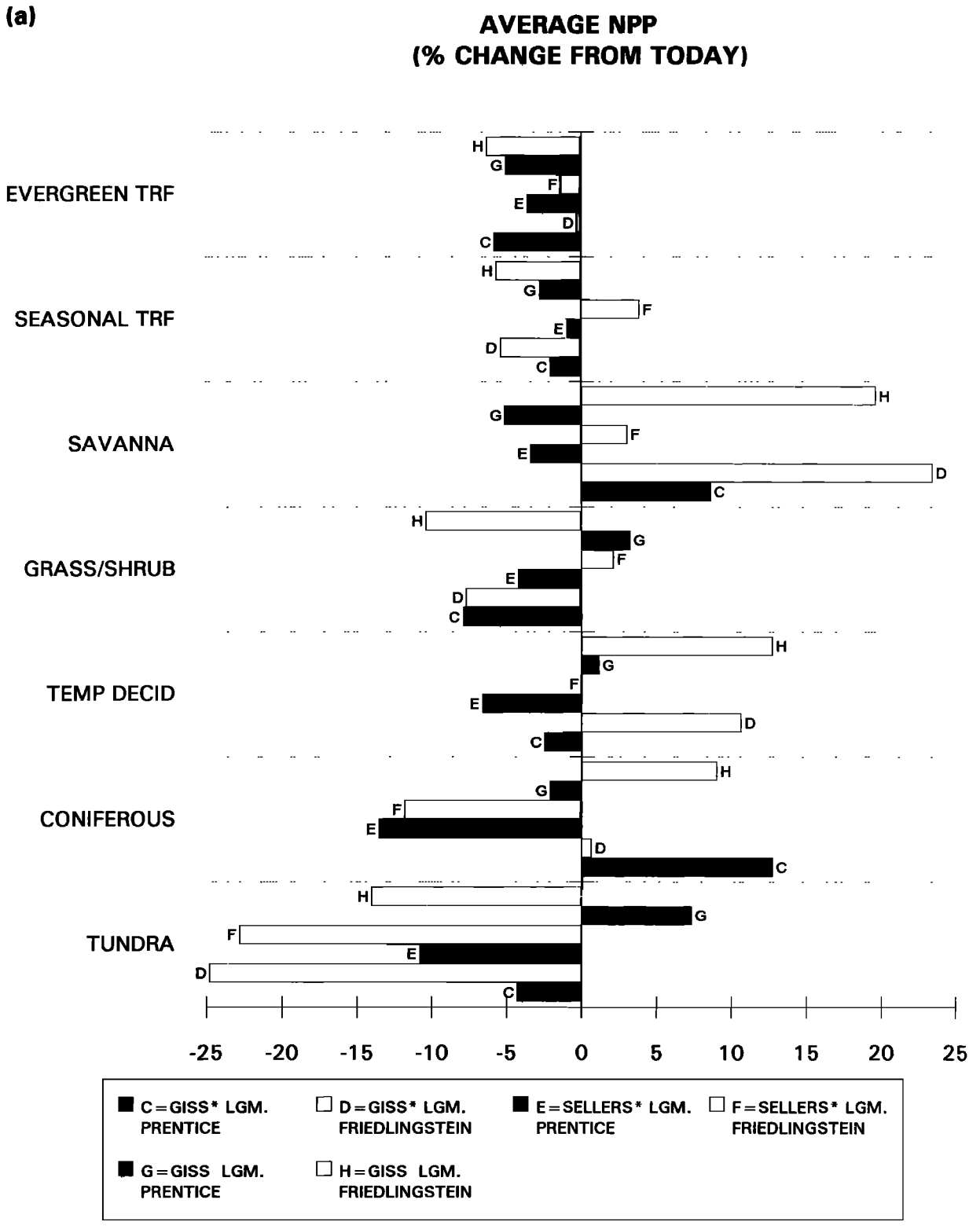

Figure 3. Relative change (LGM-today)/today in (a) NPP, (b) phytomass C density, (c) litter C density, (d) soil C density for the six climate-bioclimatic scheme experiments. Each experiment was compared to the present-day simulation using the corresponding bioclimatic scheme. Results are not shown for warm and cold deserts where the present-day values are low.

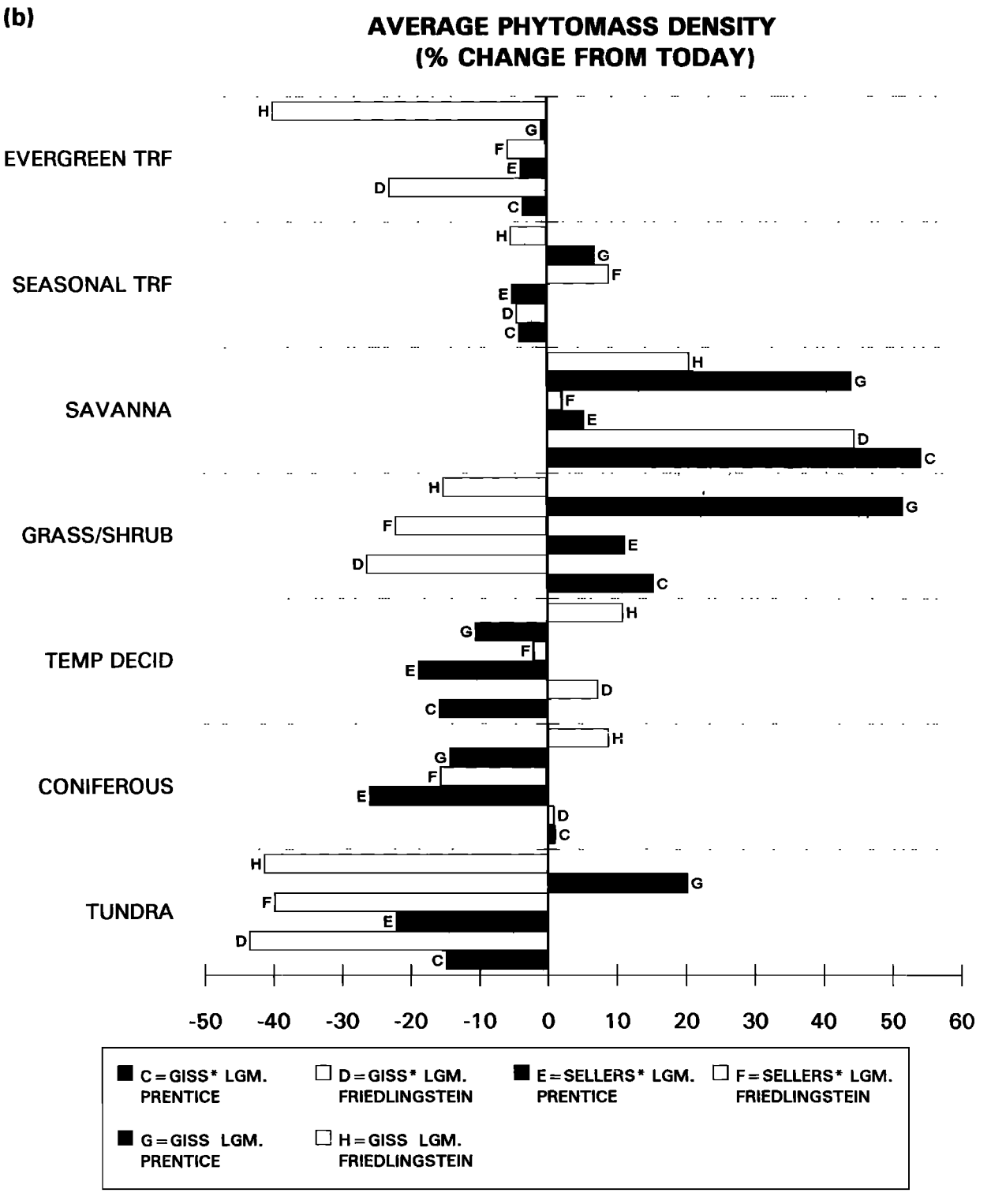

Figure 3. (continued)

climate analogs. This limitation is of importance, as recent modeling approaches have been adopted to predict the future biosphere, calculating the climatic impact on the vegetation redistribution [*Smith and Shugart*, 1993; PF90; *Henderson-Sellers*, 1993].

These results also highlight the potential problem of carbon schemes having many parameters that depend on vegetation or soil types; any calculation of changes of carbon content due to climate (e.g., LGM, $2\times CO_2$) change becomes extremely dependent of the redistributed vegetation.

Global and Local Constraints

Knowing the intrinsic limitations of our approach, the only way to narrow the uncertainty for the LGM terrestrial carbon estimate is to constrain the global carbon budget with the oceanic $\delta^{13}C$ information and the vegetation distribution with palynological information.

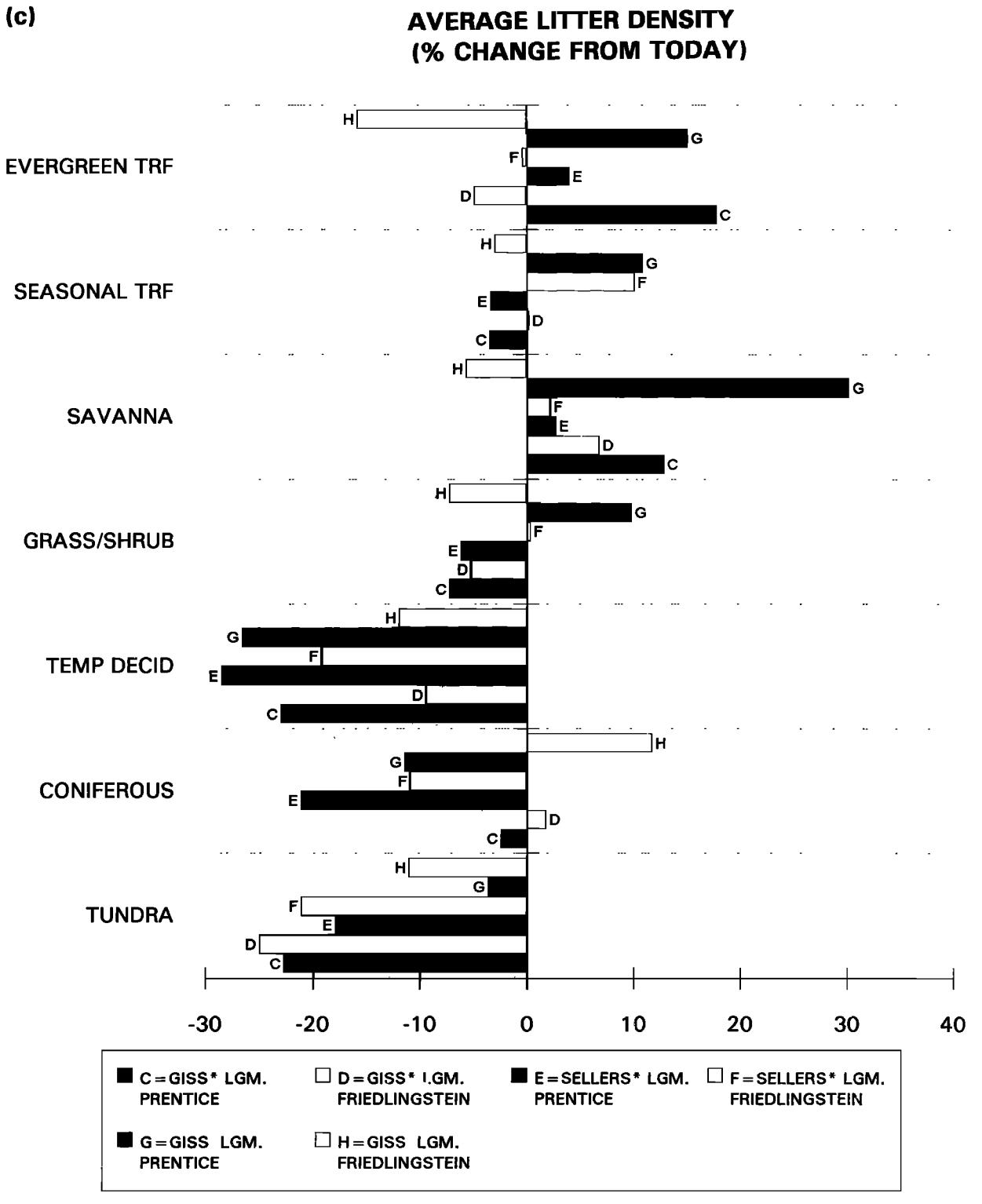

Figure 3. (continued)

As mentioned before, the GISS LGM climate gives, no matter the bioclimatic scheme, a LGM carbon content higher than today, which is total disagreement with the $\delta^{13}C$ shift. This is not surprising, as GISS LGM climate is known to overestimate the precipitation [*Rind*, 1987].

We examined LGM vegetation distributions compiled from available pollen information, specifically in the tropical regions, to try to constrain our results in these regions where the agreement between the bioclimatic schemes is the weakest.

On the northeastern coast of South America the LGM vegetation was deduced to be dry savanna [*Frenzel*, 1992], tropical forest and subtropical savanna [*Grichuk*, 1992], and tropical shrubland/woodland [*Adams et al.*, 1990]. *Clapperton* [1993] concluded that during the

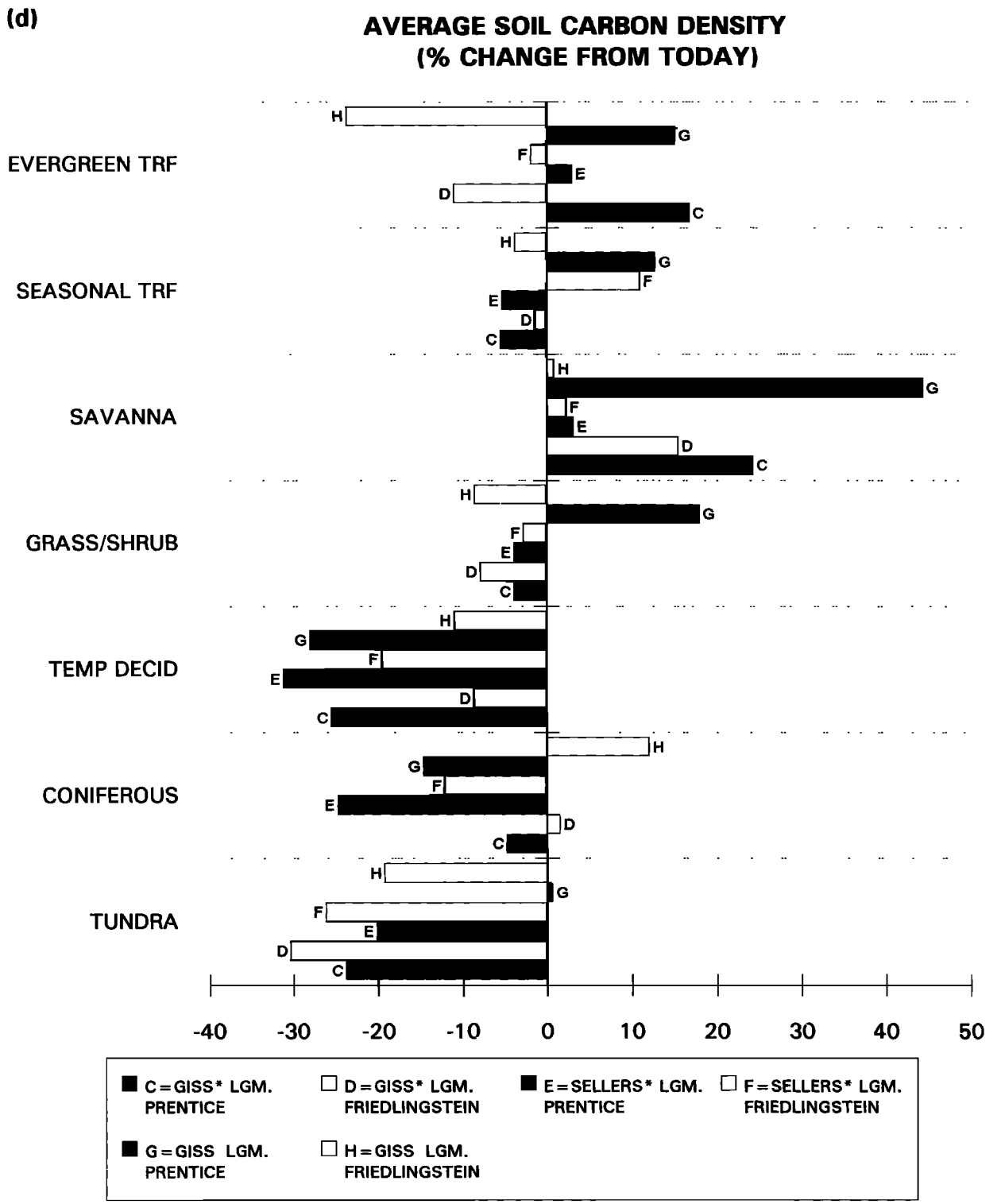

Figure 3. (continued)

LGM, savannas extended over a large portion of the area covered by tropical evergreen forests today.

Any of the South American vegetations produced with GISS LGM (and to a lesser extent with GISS* LGM) is wetter than those obtained from pollen information: Prentice's scheme predicting evergreen tropical forest and Friedlingstein's scheme modeling temperate deciduous forest.

In Southeast Asia (Malay peninsula and just north), reconstructed vegetation is tropical/subtropical mountain forest with dry savanna [*Frenzel*, 1992], tropical forest with subtropical savanna [*Grichuk*, 1992], mixed open evergreen and deciduous forests [*Velchiko and Isayeva*, 1992], tropical moist forest with some tropical shrubland and woodland [*Adams et al.*, 1990], or semievergreen rainforest and mountain vegetation [*Van*

Table 3. Same as Table 2 but for GISS* LGM, Sellers* LGM, and GISS LGM Climates

	GISS* LGM•Prentice				GISS* LGM•Friedlingstein			
Veg Type	Area, 10^6 km^2	Phyt C, Gt C	Lit C, Gt C	Soil C, Gt C	Area, 10^6 km^2	Phyt C, Gt C	Lit C, Gt C	Soil C, Gt C
1	17.5	260.5	7.4	157.8	3.0	34.3	0.9	18.1
2	10.1	105.4	3.7	72.9	2.1	23.4	0.8	15.5
3	1.2	11.5	0.4	7.8	4.9	28.6	1.3	22.1
4	47.6	94.4	12.0	179.5	39.1	31.4	10.9	140.1
5	16.2	192.8	11.4	237.3	33.6	560.6	25.2	553.6
6	12.5	116.5	11.7	239.1	13.4	133.4	15.0	311.5
7	5.5	12.5	2.4	41.0	17.9	29.0	8.5	134.4
8	12.1	7.0	1.2	18.1	16.8	1.7	0.8	9.5
9	29.8	6.7	1.8	24.9	21.8	0.5	0.3	3.3
Global	152.5	807.2	52.0	978.3	152.5	842.7	63.5	1208.0
	Sellers* LGM•Prentice				Sellers* LGM•Friedlingstein			
Veg Type	Area, 10^6 km^2	Phyt C, Gt C	Lit C, Gt C	Soil C, Gt C	Area, 10^6 km^2	Phyt C, Gt C	Lit C, Gt C	Soil C, Gt C
1	11.2	167.2	4.2	89.6	8.2	116.6	2.6	55.5
2	13.1	134.9	4.8	94.5	5.4	68.3	2.1	44.6
3	7.7	49.4	2.3	40.7	11.5	47.2	3.0	45.7
4	39.0	74.4	9.9	146.9	34.3	29.1	10.1	129.7
5	12.7	145.3	8.3	171.3	15.2	230.4	10.1	219.9
6	12.9	88.0	9.8	194.9	13.2	110.1	13.0	265.8
7	10.5	22.0	5.0	82.5	20.0	34.7	10.0	159.7
8	15.7	2.9	0.7	9.9	22.2	1.2	0.5	6.5
9	29.7	5.5	1.7	23.5	22.4	0.4	0.2	3.1
Global	152.5	689.6	46.7	853.8	152.5	638.0	51.7	930.6
	GISS LGM•Prentice				GISS LGM•Friedlingstein			
Veg Type	Area, 10^6 km^2	Phyt C, Gt C	Lit C, Gt C	Soil C, Gt C	Area, 10^6 km^2	Phyt C, Gt C	Lit C, Gt C	Soil C, Gt C
1	21.2	325.3	8.8	188.9	0.5	4.3	0.1	2.5
2	6.5	75.0	2.7	55.6	1.1	12.3	0.4	8.0
3	1.0	8.4	0.4	7.0	1.6	7.6	0.4	6.1
4	35.1	91.3	10.4	162.4	30.2	27.9	8.2	107.5
5	26.0	328.4	17.4	367.4	49.5	852.8	36.0	793.9
6	16.9	133.3	14.4	289.3	15.1	162.9	18.7	388.7
7	8.1	26.2	4.5	80.3	25.6	43.2	14.4	223.2
8	1.3	1.0	0.2	2.8	3.4	0.4	0.2	2.6
9	36.5	8.5	2.0	29.1	25.5	0.3	0.2	2.2
Global	152.5	997.3	60.8	1182.9	152.5	1111.6	78.6	1534.8

der Kaars, 1991]. In these regions, both bioclimatic schemes predict tropical evergreen forest, even with the driest climate (Sellers* LGM), not in disagreement with the pollen data.

We focused this palynological analysis in the tropical region, where the disagreement between the modeled vegetation is the largest. Unfortunately, it is also the region where the pollen data are very scarce and most divergent. Also, tropical climates simulated with the GCMs have the largest uncertainties because of the uncertainties in SSTs. As a result, except for the GISS LGM climate that always overpredicts the forest extent in the tropical band, the pollen constraint is not strong enough to eliminate one of the four remaining vegetation distributions. Therefore our first estimation of the biospheric carbon content at LGM ranges from 1590 to 2114 GtC, i.e., 313 ± 295 GtC lower than today. Nevertheless, the palynological information indicates drier vegetation types than any of our simulations. For that reason, we recalculated the carbon inventory, keeping the modeled vegetation distributions in the high- and medium-confidence regions, but replacing the modeled forest by grasslands, as observed, in the low-confidence regions. This calculation leads to a lower and narrowed estimation ranging from 1416 to 1625 GtC (611 ± 105 GtC lower than today).

Concluding Remarks

The estimate of the change of terrestrial carbon inventory for the LGM can be viewed step by step. Using different models, we first calculated a LGM carbon in-

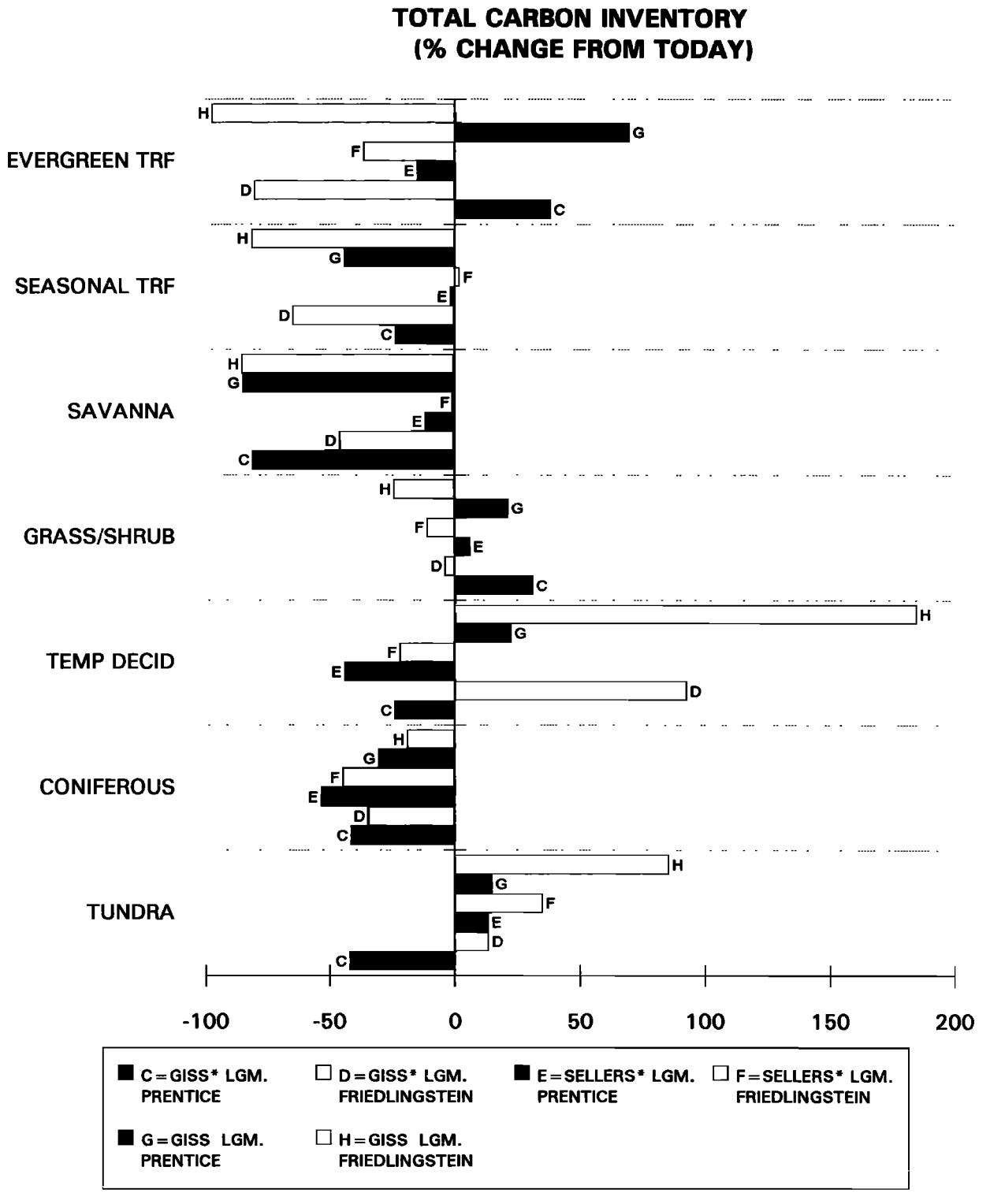

Figure 4. As Figure 3 but for total carbon inventories.

ventory of 313 ± 295 GtC lower than today (rejecting GISS LGM simulations). Replacement of the simulated vegetation types in the low-confidence regions with that deduced from palynological data results in a reestimation of the Holocene-LGM change: 611 ± 105 GtC.

Inclusion of the effects of low atmospheric CO_2 on NPP would further lower carbon storage during the LGM. A simple calculation using a β function [*Bacastow and Keeling*, 1973] shows a decrease of 11% in phytomass, litter, and soil carbon densities when atmospheric CO_2 drops from 280 to 200 ppmv. Accounting for that effect enhances the Holocene-LGM change by about 160 GtC. Furthermore, the present-day storage does not include the postglacial storage in peatlands;

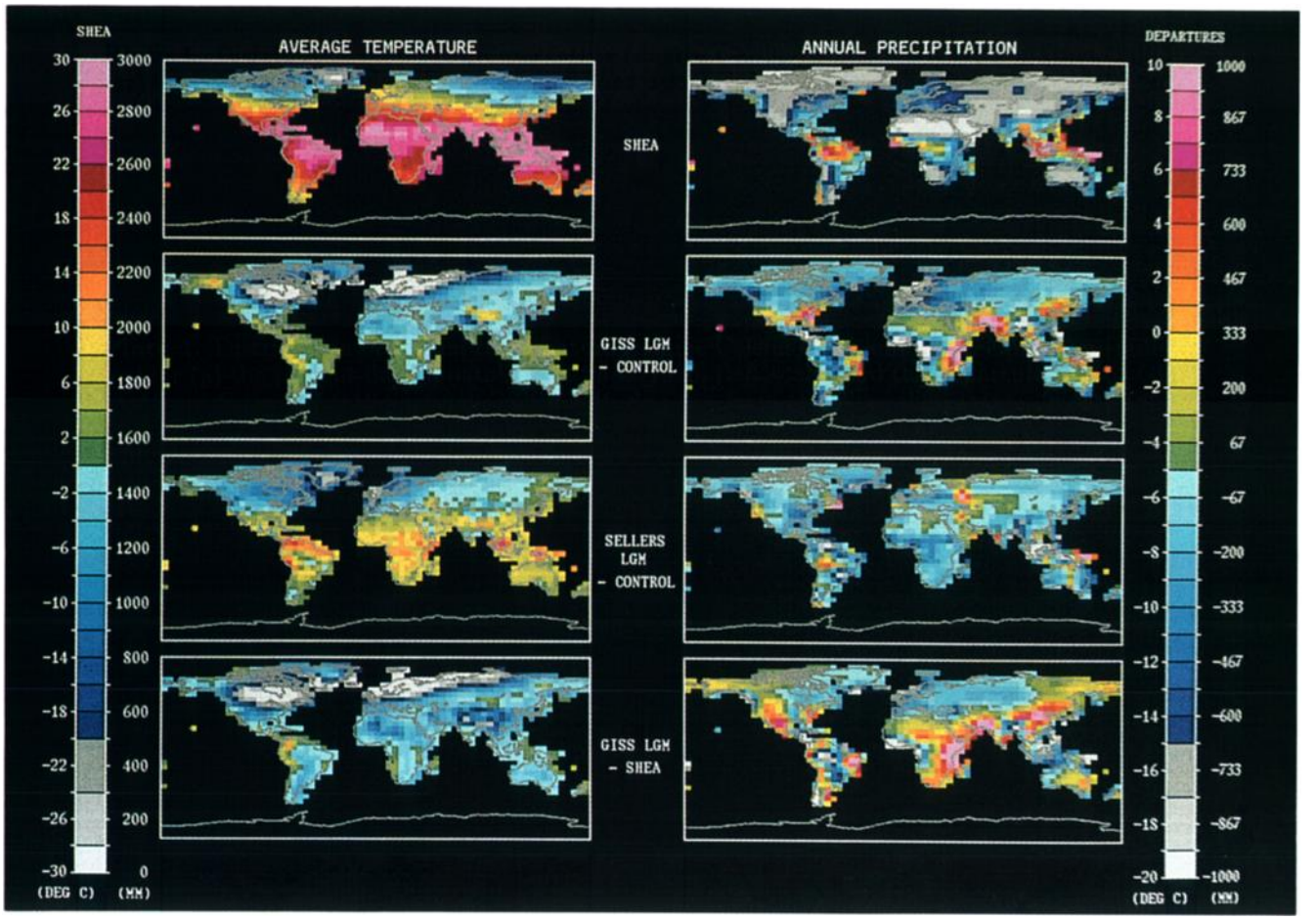

Plate 1. Distribution of annual temperature (degree Celsius) and annual precipitation (millimeter) for (a) the present-day climatology of *Shea* [1986] (left scale) and the departures of (b) GISS* LGM, (c) Sellers* LGM, and (d) GISS LGM climates from the Shea climatology (right scale).

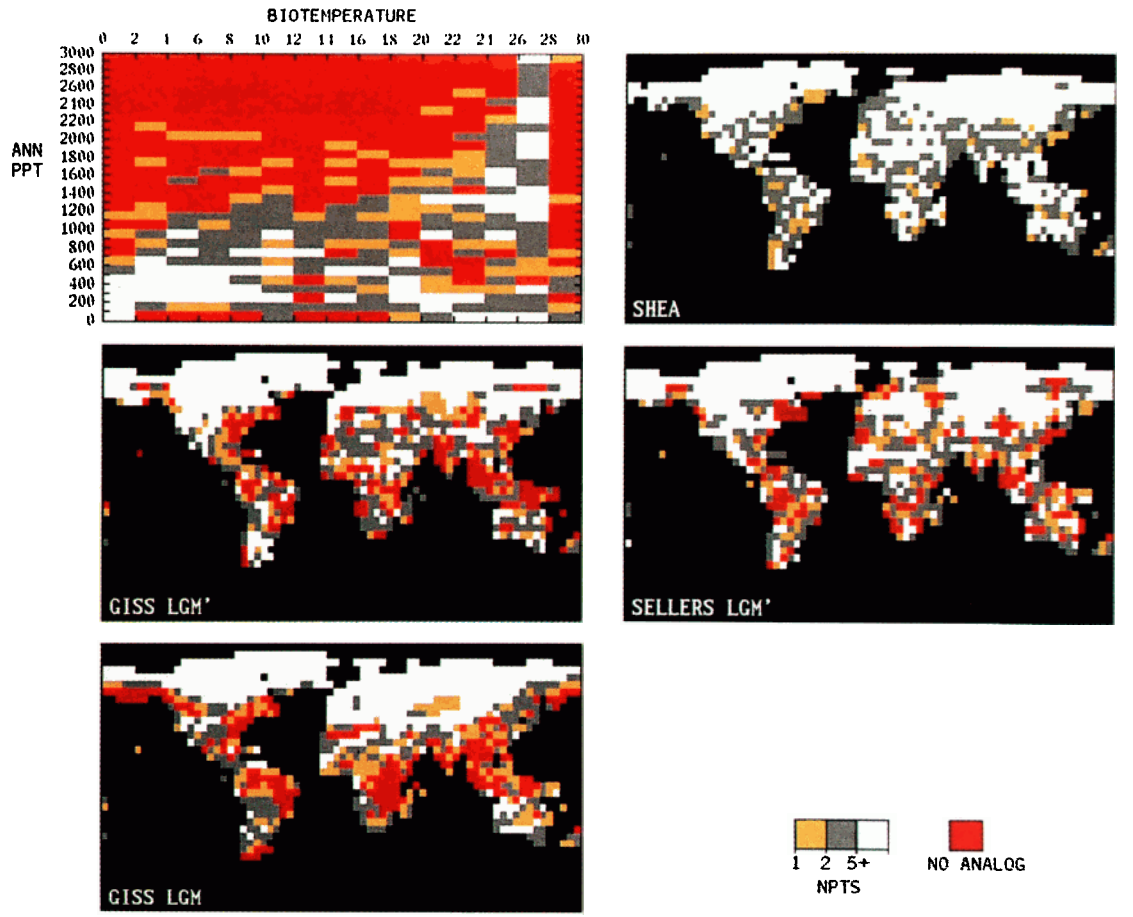

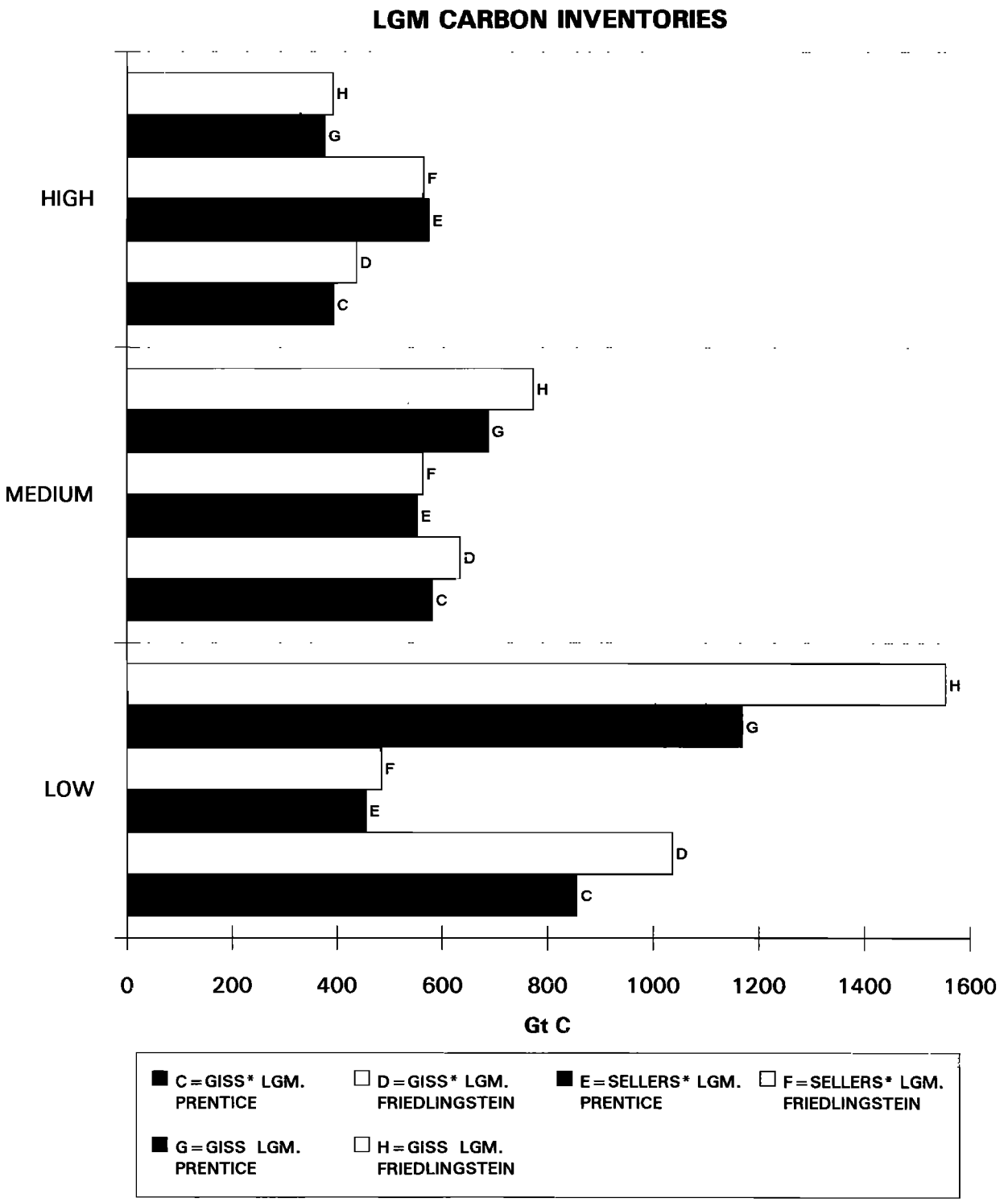

Figure 5. Total global carbon inventories in (a) high-, (b) medium-, and (c) low-confidence regions, as simulated in the six LGM experiments. Unit is gigatonnes of carbon.

Plate 2. (a) Number of 5° x 5° land grid cells that fall in each 2°C x 100 mm division of the biotemperature–annual precipitation climatic space. Bins accounting for >4, 2-4, 1, and 0 grid cells are in white, grey, orange, and red, respectively. Latitude-longitude distribution of the "common", "infrequent", "rare", and "no-analog" climate types for (b) Shea climatology, (c) GISS* LGM climate, (d) Sellers* LGM climate, and (e) GISS LGM climate. The color scheme is the same as in Plate 2a.

Harden et al. [1992] estimated a sequestration of 170 GtC after the Laurentide Ice Sheet deglaciation. Again, inclusion of this additional postglacial terrestrial carbon reservoir would increase the Holocene-LGM difference. Taking into account the fertilization effect and the postglacial peat formation leads to a LGM to present increase of 1000 GtC or so. This final estimate is much higher than the 500 GtC change deduced from the shift in the $\delta^{13}C$ of ocean sediments. The direct biospheric and the oceanic derived estimates seem even harder to reconcile if one has in mind that the 500 GTC inferred from the $\Delta\delta^{13}C$ should be seen as an upper limit. Indeed, that calculation does not include the possibility that during the postglacial sea level change, marine carbon may have been sequestered on the continental shelves, as suggested by *Broecker* [1981]. Such a mechanism would contribute to the $\Delta\delta^{13}C$ and hence reduce the magnitude of the inferred terrestrial carbon change [*Broecker,* 1981; *Knox and McElroy,* 1985].

Undoubtedly, the uncertainties associated to the additive processes mentioned above (palynological constraints, fertilization effect, peatland growth) are important. Tropical pollen, especially from the southern hemisphere is very rare; therefore the replacement of forest with grassland in the tropical regions should be seen as an extreme case. The fertilization effect was poorly parameterized in this study; it has been shown [*Melillo et al.,* 1993; *Shaver et al.,* 1992] that the impacts of climatic change and atmospheric CO_2 change on the biosphere are intimately linked, mainly through water and nutrient use efficiency feedbacks. Furthermore, very little is known about plant response to low atmospheric CO_2 as most of the CO_2 experiments are obviously concerned with elevated CO_2 levels. Also, distinction between plants having a C-3 or C-4 photosynthetical pathway can modulate the CO_2 response.

Nevertheless, it appears very hard to reconcile marine data and terrestrial model approaches, a 500 GtC being the upper limit of the first approach and also the lower limit of our modeling approach. As *Crowley* [1991] pointed out, "there is a significant gap in our understanding of ice-age terrestrial carbon storage." Analogous to the present-day CO_2 budget and its missing sink quest, this study suggests the existence of a LGM terrestrial missing CO_2 sink.

The bioclimatic schemes also play an important role, when exploring different climates. The vegetation predicted for a "no present-day analog" climate is extremely dependent on the parameterization adopted in the vegetation scheme. Consequently, large discrepancies between the vegetation (and carbon pools) predicted by different bioclimatic schemes can be expected. In a global change context, this result urges for the development of bioclimatic schemes, based on physiological properties of plants, able to model the vegetation dynamic.

Acknowledgments. We thank C. Delire for providing outputs of the Sellers global climate model for LGM conditions and J.-F. Müller and E. Matthews for particularly useful discussions. Financial support for PF comes from the Belgian Institute for Encouragement of Industrial and Agricultural Scientific Research. Part of this work is supported by NASA, Office of Mission to Planet Earth. The National Center for Atmospheric Research is sponsored by the National Science Foundation.

References

Adams, J.M., H. Faure, L. Faure-Denard, J.M. McGlade, and F.I. Woodward, Increases in terrestrial carbon storage from the Last Glacial Maximum to the present, *Nature, 348,* 711-714, 1990.

Anderson, D.M., and R.S. Webb, Ice-age tropics revisited, *Nature, 367,* 23-24, 1994.

Bacastow, R, and C.D. Keeling, Atmospheric carbon dioxide and radiocarbon in the natural carbon cycle, II, Changes from A.D. 1700 to 2070 as deduced from a geochemical reservoir, in *Carbon and the Biosphere,* edited by G.M. Woodwell, and E.V. Pecan, pp. 86-135, U.S. Department of Commerce, Springfield, Va., 1973.

Barnola, J.M., D. Raynaud, Y.R. Korotkevich, and C. Lorius, Vostok ice core provides 160,000 years record of atmospheric CO_2, *Nature, 329,* 408-414, 1987.

Broecker, W.S., Glacial to interglacial changes in ocean and atmospheric chemistry, in *Climate Variations and Variabilities: Facts and Theories,* edited by A. Berger, pp. 111-121, D. Reidel, Norwell, Mass., 1981.

Broecker, W.S., and T.-S. Peng, *Greenhouse Puzzles II, Archer's World:* CO_2 *Glacial Hideout?,* 47 pp., Lamont-Doherty Earth Observatory of Columbia University, Palisades, N. Y., and Oak Ridge National Laboratory, Oak Ridge, Tenn., 1993.

Clapperton, C.M., Nature of environmental changes in South America at the Last Glacial Maximum, *Paleogeogr., Paleoclimatol., Paleoecol., 101,* 189-208, 1993.

Climate: Long-Range Investigation Mapping and Prediction (CLIMAP) Project Members, The surface of the ice-age Earth, *Science, 191,* 1131-1137, 1976.

Crowley, T.J., Ice age carbon, *Nature, 352,* 575-576, 1991.

Duplessy, J.-C., N.J. Shackleton, R.G. Fairbanks, L. Labeyrie, D. Oppo, and N. Kallel, Deepwater source variations during the last climatic cycle and their impact on the global deepwater circulation, *Paleoceanography, 3,* 343-360, 1988.

Emanuel, W.R., H.H. Shugart, and M.P. Stevenson, Climatic change and the broad-scale distribution of terrestrial ecosystems complexes, *Clim. Change, 7,* 29-43, 1985.

Esser G., and M. Lautenschlager, Estimating the change of carbon in the terrestrial biosphere from 18000 BP to present using a carbon cycle model, *Environ. Pollut., 83,* 45-53, 1994.

Frenzel, B., Maximum cooling of the last glaciation, vegetation, in *Atlas of Paleoclimates and Paleoenvironments of the Northern Hemisphere,* edited by B. Frenzel, M. Pesci, and A.A. Velchiko, pp. 55 and 122, Geographical Research Institute, Hungarian Academy of Sciences, Budapest, 1992.

Friedlingstein P., C. Delire, J.-F. Müller, and J.-C.Gérard, The climate induced variation of the continental biosphere: A model simulation of the Last Glacial Maximum, *Geophys. Res. Lett., 19,* 897-900, 1992.

Friedlingstein, P., J.-F. Müller, and G. Brasseur, Sensitivity of the terrestrial biosphere to climate changes: Impact on the carbon cycle, *Environ. Pollut., 83,* 143-146, 1994.

Grichuk, V.P., Maximum cooling of the last glaciation, main types of vegetation, in *Atlas of Paleoclimates and Paleoenvironments of the Northern Hemisphere,* edited by B. Frenzel, M. Pesci, and A.A. Velchiko, pp. 57 and 123-124, Geographical Research Institute, Hungarian Academy of Sciences, Budapest, 1992.

Guilderson, T.P., R.G. Fairbanks, and J.L. Rubenstone, Tropical temperature variations since 20,000 years ago: Modulating interhemispheric climate change, *Science, 263*, 663-665, 1994.

Hansen, J., A. Lacis, D. Rind, G. Russel, P. Stone, I. Fung, R. Ruedy, and J. Lerner, Climate sensitivity: Analysis of feedback mechanisms, in *Climate Processes and Climate Sensitivity*, pp. 130-163, *Geophys. Monogr. Ser.*, vol. 29, edited by J. E. Hansen, and T. Takahashi, AGU, Washington, D. C., 1984.

Harden, J.W, E.T. Sundquist, R.F. Stallard, and R.K. Mark, Dynamics of soil carbon during deglaciation of Laurentide Ice Sheet, *Science, 258*, 1921-1924, 1992.

Henderson-Sellers, A., Continental vegetation as a dynamic component of global climate model: A preliminary assessment, *Clim. Change, 23*, 337-378, 1993.

Holdridge, L.R., Determination of world formations from simple climatic data, *Science, 105*, 367-368, 1947.

Knox, F., and M.B. Mc Elroy, Changes in atmospheric CO_2: Factors regulating the glacial to interglacial transition, in *The Carbon Cycle and Atmospheric CO_2: Natural Variations Archean to Present, Geophys. Monogr. Ser.*, vol. 32, edited by E.T. Sundquist, and W.S. Broecker, pp. 154-162, AGU, Washington, D. C., 1985.

Köppen, W., Das geographische System der Klimate, in *Handbuch der Klimatologie* 1, part C, edited by W. Koppen, and G. Geiger, 46 pp., Boentrager, Berlin, 1936.

Leemans, R., and W. Cramer, The IIASA database for mean monthly values of temperature, precipitation and cloudiness on a global terrestrial grid, *IIASA Res. Rep. RR-91-18*, Laxenburg, Austria, 1991.

Legates, D.R., and C.J. Willmott, Mean seasonal and spatial variability in gauge-corrected global precipitation, *Int. J. Climatol., 10*, 111-127, 1989.

Lieth, H., Modeling the primary productivity of the world, in *Primary productivity of the Biosphere*, edited by H. Lieth, and R.H. Whittaker, pp. 237-263, Springer-Verlag, New York, 1975.

Manabe, S., and R.J. Stouffer, Sensitivity of a global climate model to an increase of CO_2 concentration in the atmosphere, *J. Geophys. Res., 85*, 5529-5554, 1980.

Matthews, E., Global vegetation and land use: New high-resolution data bases for climate studies, *J. Clim., 22*, 474-487, 1983.

Melillo, J.M., A.D. McGuire, D.W. Kicklighter, B. Moore III, C.J. Vorosmarty, and A.L. Schloss, Global climate change and terrestrial net primary production, *Nature, 363*, 234-240, 1993.

Olson, J.S., J.A. Watts, and L.J. Allison, Major world ecosystem complexes ranked by carbon in live vegetation, A database, *Tech. Rep. ORNL-5862*, 164 pp., Oak Ridge Nat. Lab., Oak Ridge, Tenn., 1985.

Porter, S.C., Hawaiian glacial ages, *Quat. Res., 12*, 161-187, 1979.

Prentice, K.C., Bioclimatic distribution of vegetation for general circulation model studies, *J. Geophys. Res., 95*, 11,811-11,830, 1990.

Prentice, K.C., and I.Y. Fung, The sensitivity of terrestrial carbon storage to climate change, *Nature, 346*, 48-51, 1990.

Prentice, I.C., W. Cramer, S.P. Harrison, R. Leemans, R.A. Monserud, and A.M. Solomon, A global biome model based on plant physiology and dominance, soil properties and climate, *J. Biogeogr., 19*, 117-134, 1992.

Rind, D., Component of the ice age circulation, *J. Geophys. Res., 92*, 4241-4281, 1987.

Rind, D., The paleorecord: How useful is it in testing models for future climate prediction?, in *Global Changes of the Past*, edited by R. Bradley, pp. 398-420, UCAR OIES Global Change Institute, Boulder, Colo., 1989.

Rind, D., and D. Peteet, Terrestrial conditions at the last glacial maximum and CLIMAP sea-surface temperature estimates: Are they consistent? *Quat. Res., 22*, 1-22, 1985.

Sellers, W., A quasi three dimensional climate model, *J. Clim., 22*, 1557-1574, 1983.

Sellers, W., The effect of a solar perturbation on a global climate model, *J. Clim., 24*, 770-776, 1985.

Shackelton, N.J., Carbon-13 in Uvigerina: Tropical rainforest history and the equatorial Pacific carbonate dissolution cycles, in *The Fate of Fossil Fuel CO_2 in the Oceans*, edited by N.R. Andersen, and A. Malahoff, pp. 401-428, Plenum, New York, 1977.

Shaver, G.R., W.D. Billings, F. Stuart Chapin, A.E. Giblin, K.J. Nadelhoffer, W.C. Oechel, and E.B. Rastetter, Global change and the carbon balance of arctic ecosystems, *BioScience, 42*, 433-441, 1992.

Shea, D.J., Climatological atlas: 1950-1979, *NCAR Tech. note, NCAR TN 269 +STR*, 1986.

Smith, T.M., and H.H. Shugart, The transient response of terrestrial carbon storage to a perturbed climate, *Nature, 361*, 523-525, 1993.

Vancampo, E., J. Guiot, and C. Peng, A data-based reappraisal of the terrestrial carbon budget at the last glacial maxixum., *Glob. Planet. Change, 8*, 189-202, 1993.

Van der Kaars, W.A., Palynology of eastern Indonesian marine piston cores: A late Quaternary vegetational and climatic record of Australasia, *Paleoceanogr., Paleoclimatol., Paleoecol., 85*, 289-302, 1991.

Velchiko, A.A., and L.L. Isayeva, Maximum cooling of the last glaciation, Landscape types, in *Atlas of Paleoclimates and Paleoenvironments of the Northern Hemisphere*, edited by B. Frenzel, M. Pesci, and A.A. Velchiko, pp. 59 and 125-126, Geographical Research Institute, Hungarian Academy of Sciences, Budapest, 1992.

Woodward, F.I., *Climate and Plant Distribution*, Cambridge University Press, New York, 1987.

G.P. Brasseur, National Center for Atmospheric Research, PO Box 3000, 1850 Table Mesa Drive, Boulder, CO 80307-3000.

P. Friedlingstein (corresponding author), Belgian Institute for Space Aeronomy, 3, av. Circulaire, Brussels, 1180 Belgium.

I.Y. Fung, J.G. John, and K.C. Prentice, NASA / Goddard Institute for Space Studies, 2880 Broadway, New York, NY 10025.

(Received March 10, 1994; revised September 1, 1994; accepted November 4, 1994.)